

MoDEST: Bridging the Gap between Federated and Decentralized Learning with Decentralized Sampling

Martijn de Vos*

Delft University of Technology, EPFL
The Netherlands, Switzerland

Akash Dhasade

EPFL
Switzerland

Anne-Marie Kermarrec

EPFL
Switzerland

Erick Lavoie
University of Basel
Switzerland

Johan Pouwelse
Delft University of Technology
The Netherlands

Abstract

Federated and decentralized machine learning leverage end-user devices for privacy-preserving training of models at lower operating costs than within a data center. In a round of Federated Learning (FL), a random sample of participants trains locally, then a central server aggregates the local models to produce a single model for the next round. In a round of Decentralized Learning (DL), *all* participants train locally and then aggregate with their immediate neighbors, resulting in many local models with residual variance between them. On the one hand, FL’s sampling and lower model variance provides lower communication costs and faster convergence. On the other hand, DL removes the need for a central server and distributes the communication costs more evenly amongst nodes, albeit at a larger total communication cost and slower convergence.

In this paper, we present MoDEST: Mostly-Consistent Decentralized Sampling Training. MoDEST implements decentralized sampling in which a random subset of nodes is responsible for training and aggregation every round: this provides the benefits of both FL and DL without their traditional drawbacks. Our evaluation of MoDEST on four common learning tasks: *(i)* confirms convergence as fast as FL, *(ii)* shows a 3x-14x reduction in communication costs compared to DL, and *(iii)* demonstrates that MoDEST quickly adapts to nodes joining, leaving, or failing, even when 80% of all nodes become unresponsive.

CCS Concepts: • Computer systems organization → Peer-to-peer architectures.

Keywords: Federated Learning, Decentralized Learning, Decentralized Systems, Peer Sampling

1 Introduction

Federated Learning (FL) and *Decentralized Learning (DL)* systems enable edge devices (referred to as *nodes* in this work) to collaboratively train a global model, without sharing their local data, at reduced operating costs compared to training

within a data center. FL is nowadays used for various applications, including next-word prediction on keyboards [1, 9, 11, 16], speech recognition [48], wireless communications [10, 38], human activity recognition [50], and health applications [7, 32, 44, 47]. At the same time, DL has also increasingly gained interest for similar applications avoiding the need of a central server [23, 24, 30, 39]. The main difference between FL and DL lies in which nodes participate in training and how aggregation is performed.

In FL algorithms [35], a central server in each training round selects a *sample*, *i.e.*, a random subset of nodes, that train a model in parallel. Nodes then send their updated model to the server, which aggregates incoming models into a single model. While this aggregation step accelerates model convergence compared to DL, the communication burden is highly concentrated on the central FL server because it remains solely responsible for global coordination throughout training. Moreover, using a centralized server incurs deployment costs, may introduce a communication bottleneck [15], and its failure will compromise training progress.

In DL algorithms [23, 30], all nodes participate in each training round, both for training and aggregation. Each node maintains a local model, and every round aggregates it with the models of its *neighbours*, *i.e.*, a subset of other nodes. DL algorithms potentially have lower deployment costs, and failure of a node does not necessarily hamper progress. However, while all local models eventually converge towards the same value [23, 25], in any given round, local models may still vary significantly. Those differences, *i.e.*, the residual variance between local models after aggregation, negatively impact the convergence speed [5, 25]. Moreover, while the communication costs in DL settings are spread equally between all nodes, the participation of every node in every round results in higher communication costs than in FL.

We quantify the tradeoff between convergence speed and communication costs between FL and DL in Figure 1 and Table 1. Figure 1 shows the learning curves of a FL algorithm (FEDAvg [35]) and a DL algorithm (D-SGD [30]) on the FEMNIST dataset [8] with the absolute time on the horizontal axis. Table 1 shows the associated total communication costs, as well as the minimum and maximum network usage incurred by any participating node. Figure 1 shows

*Corresponding author. Work conducted during a research visit at EPFL.
Email: martijn.devos@epfl.ch.

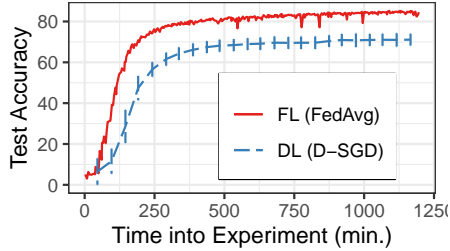


Figure 1. The model convergence of FL and DL for the FEMNIST learning task (results extracted from Figure 3c).

Dataset	Method	Total	Min.	Max.
FEMNIST	DL (D-SGD)	1004.1 GB	2.8 GB	2.8 GB
FEMNIST	FL (FedAvg)	14.1 GB	7.6 MB	7.1 GB

Table 1. The total, minimum and maximum network usage per node, for FL and DL, and with the FEMNIST dataset.

that FL converges faster than DL and also reaches higher final test accuracy. While the total network usage incurred for DL (1004.1 GB) training is 71x higher than FL (14.1 GB), the maximum network usage on any node in DL (2.8 GB) is significantly lower than in FL (7.1 GB) where the communication burden is concentrated on the server.

The tradeoff between convergence speed and communication costs may appear inherent to FL and DL but a closer inspection suggests otherwise. We therefore asked ourselves: *Can a learning algorithm obtain fast model convergence, similar to FL, with smaller total communication costs than DL, by involving only a subset of nodes at each iteration and still not rely on centralized components?*

In the rest of this paper, we answer this affirmatively. We design, implement, and evaluate MoDEST, a novel algorithm for decentralized learning, which decentralizes the random sampling approach of FL by (i) having each participant compute the next sample of active nodes independently and (ii) shift the aggregation process, traditionally done by a centralized server, to a subset of the active nodes within each sample. Since the learning process tolerates some variance between models, we allow nodes to derive slightly inconsistent samples. These inconsistencies arise when nodes are joining or leaving the network (churn), or have crashed. This allows MoDEST to forego the use of network-wide synchronization protocols or expensive consensus mechanisms, such as blockchains [3, 33, 34, 41], while providing convergence speed similar to FL. To lower the number of messages and ensure timely dissemination of network changes, we piggyback the maintenance of the network (the membership protocol) on the messages already used to transfer models between samples.

In summary, we make the following contributions:

1. We present MoDEST, a novel decentralized learning algorithm. Our algorithm combines three key components: (i) a novel sampling algorithm that guarantees mostly-consistent samples, (ii) a membership maintenance protocol that tolerates churn, and (iii) a procedure that identifies and ignores unresponsive nodes.
2. Through an extensive experimental study, performed under realistic deployment conditions, we show on four common learning tasks that our approach provides similar convergence speed to FL, and superior network load-balancing like DL. Our experiments demonstrate that membership changes in MoDEST are propagated quickly, and that this mechanism, depending on the model size, incurs marginal additional network usage on the evaluated learning tasks. Finally, our evaluation shows that MoDEST is highly resilient to nodes that might crash or become temporarily unresponsive during training.
3. We fully implement MoDEST and publish its source code in a GitHub repository.

2 Federated and Decentralized Learning

In FL and DL, nodes have private local datasets and collaborate to perform a learning task, e.g., learning a single model for classification, that performs well on the union of all nodes' local datasets. To map out the design space of learning algorithms, we describe here two commonly-used algorithms to perform this task.

Federated Averaging (FedAvg) is the main algorithm used for FL [35]. Each round, a central server selects a subset of random nodes amongst those available and sends the latest version of the global model to them. The selected nodes train the received model on their local data, and send back their updated models to the server. The server averages the updated models and sends the aggregated model to a new sample in the next round. To reduce bandwidth usage, FedAvg (i) samples only a fraction of all possible nodes every round, and (ii) allows each node to perform multiple local updates prior to sending their updated model to the server.

Decentralized SGD (D-SGD) is the main algorithm used for DL and decentralizes the aggregation responsibility onto all nodes with distributed averaging: After updating their model locally, each node averages it with their *immediate neighbours* [30]. Nodes know beforehand their neighbours, from a topology established globally prior to learning, and wait for all neighbours to have sent their model before moving to the next round. D-SGD also supports multiple local updates to reduce bandwidth usage. Compared to FedAvg, D-SGD removes communication bottlenecks by having no node averaging with more than a fixed and small subset of all nodes. However, all nodes participate every round and

the use of distributed averaging leaves residual variance between local models that biases gradient computations and slows down convergence (as shown in Figure 1).

MoDEST addresses the drawbacks of D-SGD by *decentralizing the sampling approach used by FL*.

3 Design of MoDEST: a Novel Decentralized Sampling-based Learning System

We now present the design of MoDEST (Mostly-Consistent Decentralized Sampling Training), our novel approach for federated learning in decentralized environments. We first describe our system model and assumptions in Section 3.1, provide a conceptual overview of the algorithm in Section 3.2, and then present the key components of MoDEST in the remaining sections.

3.1 System Model and Assumptions

We consider a network of n nodes that collaboratively train a global machine learning model θ in a decentralized environment. Each participating node has access to a local dataset which never leaves the participants' device. Only the model parameters are exchanged between participating nodes. We assume that each node knows the specifications of the ML model being trained, the learning hyperparameters, and the settings specific to MoDEST. This information can, for example, be made available on a web page.

Network and failure model. In contrast to a data-centre setting, model training with MoDEST proceeds in an uncontrolled decentralized environment and relies on the cooperation of potentially unreliable nodes. We assume that nodes are connected through a fully connected overlay network (*i.e.*, all nodes can communicate with each other). We outline the MoDEST membership protocol later in Section 3.4. Nodes may join or leave, intentionally or unintentionally, the network at any time. We assume that participating nodes faithfully execute the algorithm but may become unresponsive at any time during the training session. These failures might be transient in nature (*e.g.*, network packet drop, or temporary disconnection) or be more permanent (*e.g.*, a participant turned off its device). Though the computational capacities of participating nodes may vary, we assume that each node's computational resources are sufficient to reliably participate in the model training. Finally, we assume a partially synchronous network model in which the delivery time of network messages is periodically bounded [13]. As such, we can detect unresponsive nodes with timeouts during the periods of synchrony and otherwise wait until the network becomes synchronous again.

3.2 MoDEST in a Nutshell

The key idea behind MoDEST is to decentralize a FL server by replicating its aggregation and sampling responsibilities

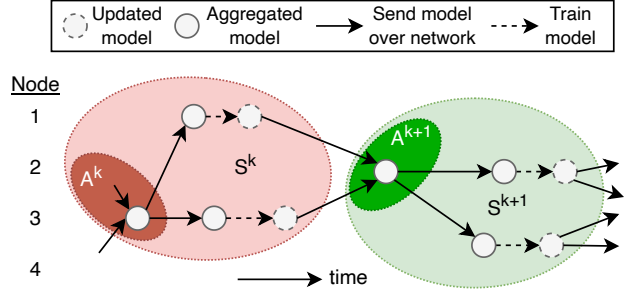


Figure 2. Overview of round k and $k+1$ in MoDEST, including 4 total nodes, a sample size of 2 ($s = 2$) and 1 aggregator ($a = 1$). For presentation clarity, we show only one aggregator - to ensure fault tolerance, a should be > 1 in deployment. Nodes 1 and 3 are in sample S^k and first train the aggregated model they received on their local data. They then send their updated model to the aggregators A^{k+1} in sample S^{k+1} . When an aggregator receives all updated models, it aggregates the incoming models and forward them to the participants in the next sample S^{k+1} .

onto nodes within each *training sample*. Similar to FL, MoDEST proceeds in rounds, and each round involves a subset of available nodes for training and aggregating models. In addition, a subset of the training sample is in charge of aggregating the local models which we refer to as *aggregators*. We refer to nodes belonging to a training sample as *participants*. These participants are randomly selected from all available nodes, with different selections every round, hence naturally balancing the computation and communication load amongst all nodes.

One of the main novelties of MoDEST is to decentralize the sampling procedure by having each participant in a sample compute the next sample independently, from their current view of the network (see Section 3.3). Each node maintains in its local view the membership and liveness information of (all) other nodes in the network. MoDEST is designed such that in most cases, node views are consistent but may be temporarily inconsistent when nodes are in the process of joining, leaving, or recently became unresponsive. Even if inconsistencies arise and participants send different updated models to distinct aggregators, this is tolerated by SGD. Therefore, MoDEST is guaranteed to converge, similar to D-SGD [31], but may do so faster because aggregation results in lower variance between models. At the same time, fixing a single aggregator for all rounds is equivalent to FL. Thus MoDEST can be viewed as the middle ground between FL and DL: nodes belonging to the training sample act as the s nodes selected by the FL server while the aggregators replace the FL server, achieving full decentralization like DL.

Figure 2 illustrates two rounds of training in MoDEST, both comprised of aggregation followed by training, when samples are consistent between participants. We show a

NOTATION	PARAMETER DESCRIPTION
s	Number of trainers in a sample.
a	Number of aggregators in a sample.
sf	Fraction of samples required for aggregation.
Δt	Timeout to detect failed nodes.
Δk	Window of activity to identify active nodes.

Table 2. The parameters used by MoDEST.

training session with a total of $n = 4$ nodes, samples of size $s = 2$, and $a = 1$ aggregators. We denote the set of nodes in the k -th sample as S^k and the subset within S^k of aggregators as A^k . In a given round k , the aggregators A^k are activated when the participants of previous sample S^{k-1} push the updated models to them. Upon aggregating, the aggregators send this model to all s participants in S^k . The participants train on their local data and further send their updated model to the next aggregators A^{k+1} as the process repeats.

MoDEST tolerates failures and ensures efficient execution in the following ways. The number of aggregators a is chosen by the system designer so that at least one reliable node is expected to participate, as it takes only one reliable aggregator to activate all reliable participants in a given round of training. Further, each aggregator requires only a fraction sf of models to be successfully received to complete aggregation. This success fraction sf also serves in reducing the impact of slow participants (stragglers). We ping candidate nodes during sampling until s have responded within a timeout Δt , to ensure the s participants were all live at the beginning of the round. We finally speed up the identification of live participants during sampling, by excluding those that were not active in the last Δk rounds.

In practical deployments, we choose the value of parameters as follows, assuming we expect at most z failures per round. These z failures include not only nodes that crash but also unresponsive nodes or nodes that experience unbounded delays in message delivery. A sample size s is chosen similar to FL [35], *i.e.* to provide the best compromise between the time required for convergence and the bandwidth used, and is dependent on the dataset and model. The number of aggregators is one more than the largest number of expected failures, *i.e.*, $a = z + 1$. The success fraction is chosen as $sf \leq \frac{s-z}{s}$ such that the aggregators can proceed with sufficient models even during failures. The sample size can be made larger and the success fraction smaller, to exclude an additional number of expected stragglers. The ping timeout Δt is chosen according to the expected upper bound on Round Trip Time (RTT) of the underlying communication network. The window of activity Δk is chosen as the best compromise between excluding unresponsive nodes as soon as possible and avoiding falsely excluding active nodes.

Table 2 summarizes the parameters of the algorithm. We analyse their impact on the system in Section 4.

In the following sections, we describe MoDEST in more detail. As there are dependencies between different parts of the algorithm, we present it progressively by focusing first on the sampling and view maintenance, and then showing how views are piggybacking on the messages related to the learning process.

3.3 Deriving Samples

The gist of MoDEST’s sampling procedure is to rely on a hash function parameterized by the round number and the node identifiers, stored by all nodes in their local view, so that each node can independently compute the sample of nodes that are expected to be active during the training. We present later how the training nodes and aggregators are selected amongst this sample. Algorithm 1 shows MoDEST sampling procedure, which aims to obtain a sample of s currently active nodes. First, a subset of *candidates* that have shown recent activity is retrieved, to avoid unnecessarily waiting for unresponsive nodes (Section 3.5). Concatenating the node identifiers with round numbers randomizes the order of nodes every round. The resulting list is sorted in lexicographic order, which provides the order in which candidates will be contacted. As long as the list of candidates is mostly consistent between nodes, the order of contact and therefore the resulting samples will also be mostly-consistent.

A candidate may have shown recent activity but still have become unresponsive in the meantime. Candidates are therefore contacted with a ping message and only those that reply with a pong message before timeout Δt will be considered. The first s candidates are all contacted in parallel to lower latency. In the best and most common case, they will all reply within Δt and the procedure can return immediately. Otherwise, remaining candidates are contacted one-by-one until enough have replied.

There might be exceptional periods in which network failures may result in all contact messages being delayed for longer than Δt . In these cases, the sampling process is repeated until the network becomes synchronous again. It may be that, upon network recovery, samples are not consistent between different nodes but they will become again in the round after.

Two rounds may overlap, and therefore the ping and pong messages from multiple rounds may be in transit concurrently. Contact messages are therefore distinguished by the sender and round in which they occur. For simplicity, implementations may also associate a unique identifier to each ping-pong exchange instead.

3.4 Joining and Graceful Leaving

MoDEST supports dynamic membership, *i.e.*, participants can join or leave while learning is already in progress. In this section, we discuss joining and the graceful leaving case, *i.e.*,

when a node successfully advertises it is leaving to at least one reliable node prior to becoming unresponsive.

Algorithm 2 shows the joining and leaving process. We defer the discussion on non-graceful cases, which are handled with activity updates in the pseudocode, until Section 3.5.

Every node maintains a *registry* that records joined and left events for all nodes including itself. This registry is stored as a dictionary E_i that associates the most recent event to each node. Each node establishes a total order between all its joined and left events, even across periods of disconnections, with a local and persistent counter c_i . This counter is independent of the rounds of learning. The counter is incremented on every join or leave event only by node i itself and therefore more recent events in the registry can only originate from node i . The updated c_i value is then associated to the corresponding event of E_i in the dictionary C_i . Only the most recent event is kept in the registry because it is the only one that is necessary to determine whether a node is currently REGISTERED, *i.e.*, its latest event being *joined*, and should be considered as a candidate for sampling.

All other nodes simply propagate the most recent event about node i , which they may have received directly from node i or indirectly from other nodes, by periodically sharing their registry, *i.e.*, the C_i and E_i dictionaries. When obtaining

Algorithm 1 Sampling of active nodes by node i .

```

1: Require: Timeout  $\Delta t$ 
2:  $L \leftarrow []$                                 ▷ Active nodes for all samples
3:
4: procedure SAMPLE( $k, s$ )
5:    $L[k] \leftarrow []$                           ▷ List of active nodes for round  $k$ 
6:   ▷ Order candidates (see Alg. 3 for CANDIDATES( $k$ ))
7:    $H \leftarrow \text{SORT}([\text{HASH}(j+k) \text{ for } j \text{ in } \text{CANDIDATES}(k)])$ 
8:   ▷ Choose the first  $s$  that are live
9:    $C \leftarrow [j \text{ for } h_j \text{ in } H]$           ▷ Candidate identifiers
10:  ▷ Optimistically ping the first  $s$  in parallel
11:  for  $j$  in  $C.\text{HEAD}(s)$  in parallel do
12:    send to  $j$  ping( $k, i$ )
13:    await pong from all  $j$  in  $C.\text{HEAD}(s)$  until  $\Delta t$ 
14:    if  $L[k].\text{SIZE} = s$  then return  $L[k].\text{HEAD}(s)$ 
15:    ▷ Sequentially add for missing responses
16:    for  $j$  in  $C.\text{TAIL}(s+1)$  do
17:      if  $L[k].\text{SIZE} \geq s$  then return  $L[k].\text{HEAD}(s)$ 
18:      else
19:        send to  $j$  ping( $k, i$ )
20:        await pong from  $j$  until  $\Delta t$ 
21:    SAMPLE( $k, s$ ) ▷ Network may be asynchronous, retry
22:
23: upon ping( $k, j$ )
24:   send to  $j$  pong( $k, i$ )
25: upon pong( $k, j$ )
26:    $L[k].\text{add}(j)$ 

```

Algorithm 2 Joining and leaving by node i .

```

1: Require: Initial random set of peers  $P \subset N$  (e.g., provided by a bootstrap server) for size  $|P| = s$ , persistent counter  $c_i$  (first initialized to 0)
2:  $E_i \leftarrow \text{DICT}()$                       ▷ Last event  $j \rightarrow \text{'joined'}$  |  $\text{'left'}$ 
3:  $C_i \leftarrow \text{DICT}()$                       ▷ Last event index  $j \rightarrow c_j$ 
4:
5: procedure REGISTERED()                    ▷ Used in Alg. 3
6:   return [ $j$  for  $j$  in  $E_i.\text{KEYS}$  if  $E_i.\text{GET}(j) = \text{'joined'}$ ]
7:
8: procedure UPDATEREGISTRY( $j, c_j, e$ )
9:   if (not  $C_i.\text{HAS}(j)$ ) or  $C_i.\text{GET}(j) < c_j$  then
10:     $E_i.\text{SET}(j, e)$ 
11:     $C_i.\text{SET}(j, c_j)$ 
12:
13: procedure MERGEREGISTRY( $C_j, E_j$ )      ▷ Used in Alg. 3
14:   for all  $j'$  in  $C_j.\text{KEYS}$  do
15:     UPDATEREGISTRY( $j', C_j.\text{GET}(j'), E_j.\text{GET}(j')$ )
16:
17: request join                            ▷ User-triggered join on  $i$ 
18:    $c_i \leftarrow c_i + 1$ 
19:   UPDATEREGISTRY( $i, c_i, \text{'joined'}$ )
20:   UPDATEACTIVITY( $i, 0$ )                  ▷ Alg. 3
21:   for all  $j$  in  $P$  do send to  $j$  joined( $i, c_i$ )
22:
23: upon joined( $j, c_j$ )                ▷ Received from node  $j$ 
24:   UPDATEREGISTRY( $j, c_j, \text{'joined'}$ )
25:    $\hat{k}_j \leftarrow \text{MAX}(N_i.\text{VALUES})$  ▷ Estimate of current round
26:   UPDATEACTIVITY( $j, \hat{k}_j$ )            ▷ Alg. 3
27:   ▷ ...Idem for leave and left( $j, c_j$ )

```

a copy of another node registry, C_j and E_j , a node uses MERGEREGISTRY to update its own registry with more recent events that may be contained in C_j and E_j .

When joining for the first time, or joining again after a disconnection, a node i first increments its persistent counter c_i , then updates its registry with a new *joined* event. It then advertises itself to a random set P with s nodes from the network, *e.g.*, obtained from a bootstrap server, with a *joined* message that includes its latest c_i counter value. Upon receiving a *joined* message from any node j , the nodes updates the corresponding registry entry for j with a *joined* event, as long as the event is more recent than the last one recorded, *i.e.*, the counter c_j for that message is larger than the last one stored. The process for leaving is essentially identical except that the event stored in the registry is *left* instead of *joined*. In both cases, if at least one node j in P is reliable and selected in a future sample k , then eventually node i should be part of the candidates for round $k+1$: Node j 's registry in sample k , which will include i 's latest event, will propagate

to the sample $k + 1$ as part of learning messages, etc. as we explain in Section 3.6.

3.5 Ignoring Unresponsive Nodes

In this section, we explain how MoDEST ignores nodes that are unresponsive even if they are registered, *i.e.*, have previously joined but not gracefully left.

The key idea is that we record the latest round of activity of a node j , as observed by the receiver of a joined or left message (Alg. 2), in a dictionary N_i , and consider j as a candidate for sampling only if j was active in the last Δk rounds. Records of activity are gossiped between nodes so that they eventually become accurate and consistent between all nodes.

MoDEST's design works because a node i accurately knows the current round k when it is actively participating in that round (see Alg. 4 lines 11 and 25 in the next section) and stores k in N_i with its own identifier. When not active in a sample, i computes an *estimate* for j , \hat{k}_j , from the maximum round it has received from any other nodes. Therefore, when node i receives a joined or left message from node j , it takes the maximum value in N_i to update the latest round of activity for node j with \hat{k}_j (Alg. 2, l. 25). Estimates \hat{k}_j can be temporarily lower than the actual current round of the network but can never be higher, similar to logical clocks [42].

Algorithm 3 shows the procedures used by other algorithms to maintain activity records and obtain a list of candidates. UPDATEACTIVITY keeps the highest round estimate \hat{k}_j observed. VIEW combines the activity records with the registry in a single *view* of the rest of the network. MERGEVIEW updates the local activity records and registry with those obtained from other nodes. CANDIDATES compute for a given round k the list of candidates that are both registered and were active in the last Δk rounds.

Recording the activity of other nodes in terms of rounds k enables the system to gracefully suspend its activity during temporary periods of asynchrony, *i.e.*, when the network may delay the messages of a large fraction of nodes beyond the timeout Δt used in sampling. In those cases, rounds will pause because less than s nodes can be selected for sampling in a given round. Once the network resumes synchrony, no activity records will have been updated with higher rounds, therefore all reliable nodes that could not communicate but can again, will still be considered as candidates.

It might also be possible that a few reliable nodes may have their messages temporarily delayed by more than Δt , then become wrongly suspected of having become unresponsive and ignored for future samples. In those cases, a user or application may simply request to join again. A node may automatically recover from those situations by recording a timestamp every time it becomes active in a sample and deduces from the difference the average time for a round,

Algorithm 3 Ignoring unresponsive nodes by node i .

```

1: Require: Window of activity  $\Delta k$ 
2:  $N_i \leftarrow \text{DICT}()$  ▷ Latest activity  $j \rightarrow \hat{k}_j$ 
3:
4: procedure UPDATEACTIVITY( $j, \hat{k}_j$ )
5:    $\hat{k}'_j \leftarrow \text{if } N_i.\text{HAS}(j) \text{ then } N_i.\text{GET}(j) \text{ else } 0$ 
6:    $N_i.\text{SET}(j, \text{MAX}(\hat{k}'_j, \hat{k}_j))$ 
7:
8: procedure VIEW()
9:   return  $(C_i, E_i, N_i)$  ▷ Combined with registry (Alg. 2)
10:
11: procedure MERGEVIEW( $V_j$ )
12:    $(C_j, E_j, N_j) \leftarrow V_j$ 
13:   MERGEREGISTRY( $C_j, E_j$ )
14:   for all  $j' \text{ in } N_j.\text{KEYS}$  do
15:     UPDATEACTIVITY( $j', N_j.\text{GET}(j')$ )
16:
17: procedure CANDIDATES( $k$ ) ▷ Recently active nodes
18:    $R \leftarrow \text{REGISTERED}()$  ▷ Alg. 2
19:   return  $[ j \text{ for } j \text{ in } N_i.\text{KEYS}$ 
20:     if  $N_i.\text{GET}(j) > (k - \Delta k)$  and  $j \text{ in } R \text{ }$ 
```

Δt_{Sk} . When a node has not received messages for more than $\Delta k * \Delta t_{Sk}$, it can request a new join to advertise itself again.

3.6 Training and Aggregating Models

In this section, we combine the mechanisms of the last three algorithms into a full learning algorithm that performs the actions as shown in Figure 2. We highlight our design choices and outline in Algorithm 4 the process of model training by participants, and model aggregation by aggregators.

To recap, every round, the participants in a sample S^k send their updated model to the aggregators in sample S^{k+1} , found using the sampling procedure of Alg. 1. Note here that the first a nodes of the hashed and sorted list H (line 7, Algorithm 1) are selected as the aggregators in the sample S^{k+1} . These aggregators then use sampling to find the rest of the participants in S^{k+1} and send them the aggregated model for training. In addition, *views* on the state of other nodes are piggybacked on the model transfer messages.

The design of the learning algorithm is based around a *push* model, in which nodes in sample S^k trigger the activation of nodes in sample S^{k+1} . This way, nodes do not have to accurately know the current round the system is in, they only have to activate when it is their turn. This also avoids the need for tuning the average time a round should take, in contrast to Gossip Learning, because a round completes as soon as all the required updates are available. Moreover, in combination with the redundancy of having multiple aggregators, this allows an aggregation step to complete as soon

Algorithm 4 Training and aggregating by node i .

```

1: Require: Number of trainers  $s$ , Number of aggregators  $a$ , Fraction of samples required for aggregation  $sf$  ( $sf > 0.5$ )
2:  $\Theta \leftarrow []$                                  $\triangleright$  List of received models
3:  $k_{agg} \leftarrow 0$                              $\triangleright$  Last aggregation round
4:  $\bar{\theta} \leftarrow \emptyset$                        $\triangleright$  Model being trained (task)
5:  $k_{train} \leftarrow 0$                            $\triangleright$  Last training round
6: if  $i$  in  $S^1$  then                       $\triangleright$  Start training if in first sample
7:    $V_i \leftarrow \text{VIEW}()$                    $\triangleright$  Alg. 3
8:   send to  $i$  train(1, RANDOMMODEL( $V_i$ ))
9:
10: upon aggregate( $k, \theta_j, V_j$ )
11:   MERGEVIEW( $V_j$ ); UPDATEACTIVITY( $i, k$ )     $\triangleright$  Alg. 3
12:   if  $k > k_{agg}$  then                       $\triangleright$  Start aggregating for sample  $k$ 
13:      $k_{agg} \leftarrow k$                        $\triangleright$  Update aggregation round
14:      $\Theta \leftarrow [\theta_j]$                    $\triangleright$  Reset list
15:   else if  $k = k_{agg}$  then                 $\triangleright$  Keep accumulating
16:      $\Theta.\text{ADD}(\theta_j)$ 
17:   if  $\Theta.\text{SIZE} \geq (sf * s)$  then  $\triangleright$  Enough models received
18:      $V_i \leftarrow \text{VIEW}()$                    $\triangleright$  Alg. 3
19:      $S^k \leftarrow \text{SAMPLE}(k_{agg}, s)$            $\triangleright$  Alg. 1
20:     for all  $j$  in  $S^k$  in parallel do
21:       send to  $j$  train( $k_{agg}$ , AVG( $\Theta$ ),  $V_i$ )
22:      $\Theta \leftarrow []$                            $\triangleright$  Reset list
23:
24: upon train( $k, \theta_a, V_j$ )
25:   MERGEVIEW( $V_j$ ); UPDATEACTIVITY( $i, k$ )     $\triangleright$  Alg. 3
26:   if  $k > k_{train}$  then
27:      $k_{train} \leftarrow k$                        $\triangleright$  Update training round
28:     CANCEL( $\bar{\theta}$ )                       $\triangleright$  Cancel uncompleted training
29:   if  $k = k_{train}$  and not PENDING( $\bar{\theta}$ ) then
30:      $\bar{\theta} \leftarrow \text{async TRAIN}(\theta_a)$ 
31:     await  $\bar{\theta}$ 
32:     if not CANCELED( $\bar{\theta}$ ) then
33:        $\theta_i \leftarrow \text{RESULT}(\bar{\theta})$            $\triangleright$  New model
34:        $V_i \leftarrow \text{VIEW}()$                    $\triangleright$  Alg. 3
35:        $A^{k+1} \leftarrow \text{SAMPLE}(k_{train} + 1, a)$      $\triangleright$  Alg. 1
36:       for all  $j$  in  $A^{k+1}$  in parallel do
37:         send to  $j$  aggregate( $k_{train} + 1, \theta_i, V_i$ )

```

as one aggregator completed, providing automatic selection of the fastest path with no extra mechanism.

Each node implements two concurrent tasks: one for aggregation and one for training. This design is necessary because a node may be concurrently training in a sample S^k and aggregating in a sample S^{k+1} at the same time: failing to complete the training step may prevent the aggregation step from reaching sf models, therefore stalling progress. Each task therefore maintains a separate round number, respectively k_{agg} and k_{train} . The round numbers are first used to

interrupt pending tasks if the network has got ahead: aggregation, respectively training, is interrupted if the same task is triggered with a higher round number. Liveness is guaranteed if at least one aggregator is reliable. When a node is aggregating and receives an aggregate message with a higher round number, it implies the previous aggregation succeeded. Moreover, receiving a training message with a higher round number also implies the aggregation step in-between succeeded. Similarly, the round numbers are also used to ignore stale messages. If an aggregate or a train message for round k arrives while a node is in round $k' > k$, then it implies the previous aggregation succeeded, and the message can be safely ignored.

The maintenance of network views V_i , comprised of the registry (Alg. 2) and the records of last activity (Alg. 3), is piggybacked onto the model transfers in aggregate and train, and only transferred with those. Since the models are typically several times larger than the views, this adds limited overhead and avoids extra messages. This is possible because the only nodes that require accurate information about the network are the active nodes in sample S^k , when they are computing nodes for sample S^{k+1} . Because samples are randomized uniformly (Section 3.3), any reliable node in the network should be selected every $\frac{n}{s}$ samples on average, which also gives the average period with which a node will refresh its view with that of other nodes. The consequence is that nodes that are not currently active in a sample can only derive an *estimate* of the current round (Section 3.5).

For presentation clarity and implementation simplicity, sampling is only triggered once aggregation or training has succeeded. It is possible to trigger sampling at the beginning instead to make it concurrent and accelerate the system.

4 Implementation and Experimental Evaluation

We now describe our implementation and present the experimental evaluation of MoDEST on our compute cluster.

4.1 Implementation Details

We implement MoDEST in the Python 3 programming language, spanning a total of 3'812 lines of source code (SLOC). MoDEST leverages the IPv8 networking library [51] which provides support for authenticated messaging and building decentralized overlay networks. Network communication in MoDEST proceeds using the stateless UDP protocol, for efficiency reasons and to avoid maintaining open connections with potentially many nodes. Since IPv8 does not provide support for bulk data transfers over UDP (needed to exchange ML models between nodes), we implemented the Trivial File Transfer Protocol (TFTP) [49]. Our implementation adopts an event-driven programming model with the `asyncio` library. We use the PyTorch library [40] to train ML

DATASET	TASK	NODES	LEARNING PARAMETERS	MODEL	MODEL SIZE
CIFAR10 [27]	Image classification	100	$\eta = 0.002$, momentum = 0.9	CNN (LeNet [18])	346 KB
CelebA [8]	Image classification	500	$\eta = 0.001$	CNN	124 KB
FEMNIST [8]	Image classification	355	$\eta = 0.004$	CNN	6.7 MB
MovieLens [14]	Recommendation	610	$\eta = 0.2$, embedding dim = 20	Matrix Factorization	827 KB

Table 3. Summary of datasets used to evaluate MoDEST.

models. Our implementation is open source and all artifacts are published in a GitHub repository.¹

We envision that organizers set up a *training session* when they wish to train a ML model in a particular application domain, such as image classification or text prediction. This happens out-of-band of MoDEST. For example, organizers can recruit volunteers who are willing to donate their resources to collaboratively train the machine learning model. To address a Sybil Attack [12], *e.g.*, the situation where an adversary joins the network under many fake pseudonyms to disrupt the training process, we assume that participation in a training session is explicitly approved by organizers, *e.g.*, using digital signatures. Volunteers download and install the MoDEST software, and start to participate by downloading metadata required for a particular training session. This metadata includes the learning parameters, model specifications, and the system parameters listed in Table 2, and should be made publicly available by the organizers.

4.2 Experiment Setup

We describe our experiment setup, datasets, and parameters.

Environment. We run all experiments on machines in our compute cluster. Each machine is equipped with dual 24-core AMD EPYC-2 CPU and 128 GB of memory, running CentOS 8. Since we envision that MoDEST will be used in WAN environments, we add latency to outgoing network traffic at the application layer. To this end, we collect ping times from WonderNetwork, providing estimations on the RTT between their servers located in 277 geo-separated cities [52]. After data cleaning, we are left with a complete latency matrix for 227 cities worldwide. When starting an experiment, we assign peers to each city in a round-robin fashion and delay outgoing network traffic accordingly.

In Section 4.3 we compare MoDEST with FL and DL. Since we do not have sufficient physical resources to conduct real-time DL experiments, and to ensure a fair comparison between different learning approaches, we simulate the passing of time in our experiments. We achieve this by customizing the default event loop provided by the `asyncio` library. This requires minimal changes to the code. We have also verified with smaller-scale experiments that we obtain similar conclusions when running experiments in real-time.

¹Link omitted due to double-blind review.

Datasets. We evaluate MoDEST on different models on four distinct datasets, whose characteristics are displayed in Table 3. The CIFAR10 dataset [27] is IID partitioned by uniformly randomly assigning data samples to nodes. This results in each node being assigned an equal number of data samples per class. The CelebA and FEMNIST datasets are taken from the LEAF benchmark [8], which was specifically designed to evaluate the performance of FL tasks in non-IID settings. To study these datasets in the DL settings, we distribute subsets of FL clients equally amongst the chosen number of nodes in the DL setup. Lastly, we also study a recommendation model based on matrix factorization [26] on the MovieLens 100K dataset [14], comprising user ratings for several movies. Here, we consider the one-user-one-node setup, imitating the realistic scenario where individual participants may wish to learn from others' movie preferences. Our evaluation thus covers a variety of learning tasks and data partitions.

Performance metrics and hyperparameters. We measure the performance of the model on a global test set unseen during training, available at each node for the purpose of evaluation. For the image classification tasks, we report the average test accuracy while for the recommendation task we report the mean squared error (MSE), indicating the difference between the actual and predicted ratings. For all the experiments, we fix the batch size $B = 20$ and we do a single pass over the local dataset each round ($E = 1$), in line with FedAvg. All models are trained using the SGD optimizer. All our learning parameters were adopted from previous works [5, 8] or were considered after trials on several values. They yield acceptable target accuracy for all datasets included in our evaluation.

4.3 The Convergence of FL, DL and MoDEST

We now analyse the performance of model training in FL using the FedAvg algorithm, in DL using the D-SGD algorithm, and MoDEST, for all learning tasks listed in Table 3.

Setup. To emulate FL using our implementation, we use $a = 1$ and fix the aggregator node, *i.e.*, nodes do not invoke the sampling function in Algorithm 1. We fix the node with the lowest median latency to other nodes to be the aggregator, to resemble the situation where a practitioner would deploy a well-connected server. We assume unlimited bandwidth capacity for the aggregator node in a FL setting. Since this experiment assumes that all nodes are reliable, we fix $sf = 1$.

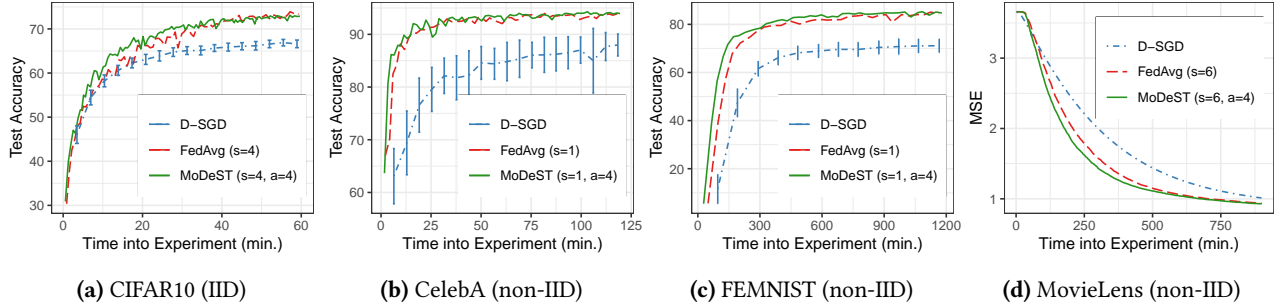


Figure 3. The model convergence for different datasets when training with FedAvg (FL), D-SGD (DL), and MoDeST.

We also implement DL in which nodes train the model every round and share their models with neighbouring nodes. We use a one-peer exponential graph topology as described in [53], which is considered state-of-the-art in this domain. This topology provides fast propagation of updates through the entire graph with low variance between local models after aggregation for fast convergence. In this topology, each node receives and sends exactly one model every round. A peer is connected to $\log(n)$ neighbours, where n is the total network size, and cycles through them in a round-robin fashion. We do not consider the cost of establishing and maintaining the graph topology, which requires global coordination to spread edges exactly evenly between all nodes. Actual deployments of D-SGD using exponential graphs would therefore have higher communication costs and latency than we report; the use of other topologies that do not require global coordination would have slower convergence speed.

For FEDAVG and MoDeST, we report the accuracy/MSE of the global model. For D-SGD we report the mean and standard deviation of the accuracy obtained by evaluating models of individual nodes on the test dataset. However, for the MovieLens dataset in D-SGD, we report the MSE of the average model across nodes. Since we use the one-user-one-node setup in the non-IID partitioning of the MovieLens dataset, many users have missing embeddings for many movies which results in arbitrarily high losses on the global test if the prior approach of evaluating individual models is used. Lastly, we also search for the sample size that results in the lowest time until a target accuracy or MSE value is reached. We then evaluate both FEDAVG and MoDeST for this value of s .

Results. Figures 3a-3d depict the model performance as the experiment progresses. The time into the experiment is denoted on the horizontal axis and the model performance is on the vertical axis. All datasets and considered values of s and a result in well-trained models with comparable final accuracy/MSE.

On all four learning tasks, we observe that MoDeST performs as good as FEDAVG and much better than D-SGD (Figures 3a to 3d). D-SGD results in higher variance across

models when the datasets are non-IID (CelebA and FEMNIST datasets) than the IID case (CIFAR10) which explains the slow convergence. Since we plot the performance of the average model across nodes for the MovieLens dataset, no variance is shown. Nevertheless, the convergence trend is similar to the rest of the learning tasks. We notice that the replicated aggregators have a positive impact on model training as evidenced by the slightly faster convergence of MoDeST than FEDAVG. We explain this as follows: with $a = 1$, the participants can begin training only after they receive the aggregated model from this single aggregator. With $a > 1$, the training by participants is triggered when they receive a model from *any* aggregator, which are sending models *in parallel* to the participants. The automatic selection of the fast path (see Section 3.6) reduces the overall round time when models take more time to be transferred. This demonstrates that MoDeST can speed up the entire training process by parallelizing the model transfers through multiple aggregators.

Dataset	Method	Total	Min.	Max.
CIFAR10	D-SGD	16.9 GB	169.0 MB	169.2 MB
	FedAvg	1.3 GB	2.8 MB	656.5 MB
	MoDeST	5.7 GB	30.4 MB	95.5 MB
CelebA	D-SGD	67.8 GB	135.4 MB	135.6 MB
	FedAvg	1.1 GB	0.2 MB	562.2 MB
	MoDeST	5.0 GB	1.7 MB	17.2 MB
FEMNIST	D-SGD	1004.1 GB	2.8 GB	2.8 GB
	FedAvg	14.1 GB	7.6 MB	7.1 GB
	MoDeST	68.1 GB	53.6 MB	413.6 MB
MovieLens	D-SGD	1305.6 GB	2.1 GB	2.1 GB
	FedAvg	25.3 GB	8.9 MB	12.6 GB
	MoDeST	113.5 GB	22.8 MB	292.3 MB

CIFAR10	CelebA	FEMNIST	MovieLens
124.7 MB (2.2%)	1.1 GB (22.2%)	268.8 MB (0.4%)	5.9 GB (5.2%)

Table 4. The total, minimum and maximum network usage per node (top table) and overhead of MoDeST as part of the total network usage (bottom table), for the experiments in Section 4.3. The maximum network usage is incurred by the server node in FEDAVG. The overhead consists of all additional bytes used beyond model transfers.

4.4 Network Usage and Overhead of MoDEST

The top table in Table 4 shows the network usage (incoming plus outgoing network traffic) observed during the experiments described in Section 4.3. We show the total traffic, and the minimum and maximum network usage across all nodes. Table 4 shows that for FEDAVG the single aggregator incurs roughly 50% of the total network usage (Max. vs Total). Table 4 also reveals that there is about 4.5 \times increase in network usage with using MoDEST instead of FEDAVG. At the same time, *total network usage of MoDEST is more evenly spread over active nodes compared to FEDAVG*, as indicated by a lower absolute difference between the minimum and maximum number of per node. MoDEST therefore exhibits superior load balancing compared to when using FEDAVG. Network usage is very equalized for D-SGD but at the same time, D-SGD has a 13x-71x higher communication cost compared to FEDAVG, and 3x-14x compared to MoDEST. We do note that network traffic in MoDEST has a bursty pattern: network activity temporarily increases when a node is selected as aggregator in a round.

The bottom part of Table 4 shows the overhead of traffic related to MoDEST. The magnitude of MoDEST-related traffic mainly depends on the sample size and the number of nodes in the views, e.g., a larger sample size results in more PING and PONG messages being sent. We noticed that the size of PING and PONG messages in the total MoDEST overhead is small, e.g., for FEMNIST, this number is only 1.1%. The main network usage of MoDEST originates from sending views between samples alongside models. Yet, Table 4 shows that for FEMNIST, MoDEST only *increases network traffic by 0.4%*, with the overhead decreasing proportionally to the increases in the model size. While the MoDEST network overhead is 22.2% for CelebA, we also remark that the model size of this learning task is relatively small and the number of participating nodes is high, resulting in larger views to be transferred. To further reduce bandwidth requirements of MoDEST one can, for instance, use compression techniques or selectively share entries in the views between samples.

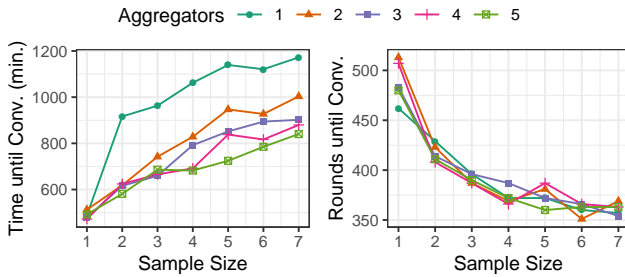


Figure 4. The time (left) and rounds (right) until convergence of MoDEST for the FEMNIST dataset over different values of s and a . The target accuracy for convergence is set to 83%.

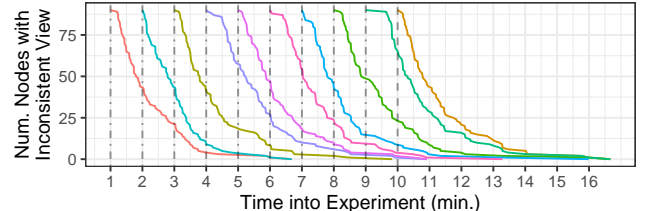


Figure 5. The number of nodes that do not have the membership information of a newly joined node as the experiment progresses. A total of ten nodes join the experiment at one-minute intervals (indicated by vertical dashed lines).

4.5 The Effect of a and s on Model Convergence

We now explore the effect of a and s on the model training.

Setup. For this experiment, we focus on the FEMNIST dataset and use MoDEST to train the model using different combinations of s and a . For each run we track the required time and number of rounds until the global model reaches a test accuracy of 83%.

Results. Figure 4 shows the time until convergence (left figure) and rounds until convergence (right figure), with the sample size s on the horizontal axis and the number of aggregators a as group variable. As s increases, the time until convergence also increases. When fixing $a = 4$, this convergence time nearly doubles when increasing s from 1 to 7: from 7.8 hours to 14.7 hours. This is because it becomes more likely that slower nodes with higher individual training times are included in the sample, thus prolonging the round time. However, the right plot in Figure 4 reveals that the number of rounds required for convergence lowers as s increases, but this effect diminishes for $s > 4$. As such, *the marginal benefits of increasing s on model convergence seems to decrease*. This matches the results that were reported by McMahan *et al.* [35] during evaluation of the FEDAvg algorithm.

Figure 4 also shows that increasing a lowers the time-to-accuracy. This is thanks to the “fast path effect” that we described in Section 4.3. With $s = 7$, the time until convergence reduces from 19.5 hours to 14 hours when increasing a from 1 to 5, a reduction of 28.3%. At the same time, the number of rounds until convergence is indifferent to an increase of a . This is because we fixed $sf = 1$ so aggregators in the same round will receive similar models and produce the same aggregated model.

4.6 Dynamic Membership and View Inconsistencies

We next focus on the ability of MoDEST to deal with inconsistent samples, caused by new nodes joining an ongoing learning session. Specifically, we quantify how the views of different nodes are updated as the experiment progresses.

Setup. We start an experiment with 90 active nodes initially. We train a CIFAR10 model with IID data distribution where the round times are of similar and predictable duration.

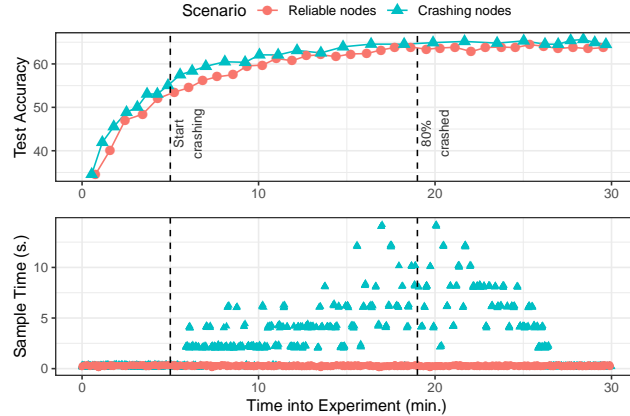


Figure 6. The model convergence and sample time with MoDEST, with and without crashing 80% of all nodes. We annotate when we start and finish crashing nodes.

Every minute, one new node joins the experiment and announces its membership by disseminating a joined message to s nodes. This repeats until there are 100 nodes participating. The first node joins a minute after the experiment started, and the last node joins ten minutes into the experiment. During the experiment, we track all view changes of nodes and set $s = 10$, $a = 5$, and $sf = 0.9$.

Results. Figure 5 visualizes how view inconsistencies are resolved after a new node joins the network. The horizontal axis denotes the time into the experiment (in minutes) and the vertical axis indicates how many of the initially joined nodes have not included a newly joined node in their view, for different join events. We annotate the time when a new node joins with dashed line. Each coloured line in Figure 5 starts at 90 and when it reaches 0, all nodes have the identity of the newly joined node j in their local view and can consider j as candidate in their derived samples. We observe that the membership status of a node i spreads quickly, and diminishes as more nodes start to know about i . For this experiment, *it takes 6.9 minutes, or roughly 56 rounds on average after a join event of newly joined node for its membership to be registered by all other nodes*. This number is independent of the number of concurrent join events. We remark that the speed of membership propagation depends on the average round duration, the total population n , and the sample size s . Specifically, it will on average take $\frac{n}{s}$ rounds for a node to be active in a sample and to know about newly joined nodes.

4.7 Handling Unresponsive Nodes

We now analyse how MoDEST handles unresponsive nodes.

Setup. We use the same dataset and parameters as the experiments in Section 4.6. We evaluate MoDEST under two scenarios. The first scenario, referred to as “reliable nodes”, involves 100 nodes while only 20 nodes being active during the entire experiment. In the second scenario, referred to

as “crashing nodes”, we start with 100 active nodes and five minutes into the experiment, we start crashing five nodes every minute. This process repeats until 80% of all nodes have crashed, *i.e.*, there are only 20 active nodes left. Since this experiment involves failing nodes, we set the ping timeout $\Delta t = 2$, which is above the maximum pair-wise network latency between nodes. We also fix the inactivity window $\Delta k = 20$ which corresponds to $2 * \frac{n}{s}$. We run the experiment for a duration of 30 minutes.

Results. The top-most plot in Figure 6 shows the model accuracy as the experiment runs. We indicate with vertical dashed lines the timestamps when we start crashing nodes and when 80% of all nodes have crashed. We also indicate in Figure 6 every fifth training round with a marker. In the “crashing nodes” scenario we observe that the round time increases after we start crashing nodes, and lowers again after roughly 26 minutes. This is caused by nodes becoming unresponsive: since they do not respond to PING messages, they delay the time it takes for nodes to determine the next sample, *i.e.*, the time it takes to complete the SAMPLE procedure (see Alg. 1). We plot the sample time in the bottom-most plot in Figure 6 and observe indeed an increase between 5 and 26 minutes into the experiment. After 26 minutes, the round and sample times become low again: unresponsive nodes are flagged as inactive and will not be pinged. The plot also shows that we achieve a slightly higher test accuracy in the scenario with crashing nodes. This is because the model updates produced by nodes before they crashed still benefit the final global model. This experiment shows that MoDEST adapts to unresponsive nodes and keeps making progress, even when a large fraction of nodes becomes unresponsive.

5 Related Work

We present work that inspired or is related to MoDEST.

Federated and Decentralized Learning. Federated Averaging [35], commonly associated to FL, is arguably the most popular algorithm for distributed learning today. Compared to a naive parallelization of SGD over multiple machines, it lowers communication requirements by sampling only a subset of nodes every round and let the nodes do multiple local updates before aggregation. The speed of convergence obtained in having a single and consistent sample inspired the design of MoDEST. Decentralized Learning techniques predate Federated Averaging by several years, but have comparatively received less attention from researchers, with somewhat of a renaissance lately. We present key ideas from those that are related to our design.

D-PSGD [30], also known as D-SGD, showed theoretically and empirically that under strong bandwidth limitations on an aggregation server in a data center, decentralized algorithms can converge faster because their rounds can

complete faster. Assumption on the behaviour of those algorithms make them mostly suited to data centers and empirical evaluations have not considered churn during training.

Gossip Learning (GL) [39] predates D-PSGD and works in more challenging environments than a data center. Comparisons between FL and GL [17] have shown that GL is competitive and sometimes has faster convergence than FL, even when deployed in a wide range of realistic scenarios. Notably, GL piggybacks peer sampling [20] information with the transmission of models, a technique also used by MoDEST. However, GL requires tuning the expected duration of a round to be large enough to allow all participants to complete training while avoiding idle time. In contrast, MoDEST immediately starts the next round when sufficient nodes are done, regardless of the values of parameters chosen (Table 2).

MoshpitSGD [45] uses a DHT to randomly combine nodes in multiple disjoint groups every round for fast averaging convergence. It is in effect an optimized version of Gossip Learning that lowers variance between models with a more efficient averaging scheme. In contrast to MoDEST, all nodes are active every round and the maintenance of the DHT does not benefit from piggybacking on the learning messages.

The impact of variance between models, that is intrinsic to DL, has been formalized as *consensus distance* [25]. When that distance is kept sufficiently low, decentralized training can converge as fast as centralized training, which can explain why even though fewer nodes are being active in FL, the network converges faster than DL.

D-Cliques [5] uses sampling to create multiple cliques of nodes such that their joint local distributions is representative of the global distribution. The benefits of clustering on convergence speed in D-Cliques motivated the initial exploration of decentralized sampling. Contrary to D-Cliques, MoDEST’s samples are randomized every round and only a single cluster is active at a time.

Advancements in FL algorithms. Lately, Asynchronous FL (AsyncFL) training [19, 37] has been shown to achieve enhanced scalability with several hundreds of concurrently training clients. While AsyncFL relieves some of the bandwidth requirements of the central server as different clients return model updates at different points in time, it still relies on the coordination through a central server, the need of which is obviated by MoDEST. More recent work on FL employs guided participant selection to improve time-to-accuracy based on statistical and systems utility of the participating clients [28]. These approaches rely on in-situ gathering of additional information about clients which is updated over training rounds. MoDEST can be extended to gossip such information along with the membership views. However, we leave the in-depth exploration of these ideas for future work. We also note that state-of-the-art FL algorithms including FEDPROX [29], FEDYOGI [43], FEDADA GRAD [43], etc. are directly implementable in MoDEST since they only require a modification to the training procedure. For instance,

to run FEDYOGI in MoDEST, participants would continue to use vanilla SGD while aggregators would use the Yogi optimizer to perform the aggregated model update. In summary, the design of MoDEST can accommodate several variants of FL training without the need for a central server.

Blockchain-Assisted Machine Learning. There have been various suggestions to decentralize the server used in FL settings using distributed ledger technology, or blockchains [21, 22, 36]. We identified various works that implement and evaluate blockchain-based learning systems [3, 33, 34, 41]. A key concern when using consensus-based replicated ledgers to coordinate learning tasks is that global consensus primitives are too strong for what is actually needed for training models. Machine learning optimization based on Stochastic Gradient Descent (SGD) is naturally resistant to failures and temporary inconsistencies, because the models will be “pulled” towards local minima that provide similarly high accuracy, even if failures or errors may shift their weights in any given round. Convergence proofs for learning algorithms show that this remains true even if averaging of models does not result in a single global model every round [31, 39]. Any design which instead tries to provide consistency, *i.e.*, enforcing that all nodes work from the same model, using consensus from an external mechanism, such as a blockchain, is bound to induce significant and unnecessary overhead.

Yet, distributed ledger technology may still provide complementary benefits when combined with learning systems without reaching consensus. For example, maintaining a DAG with model updates can help to detect model poisoning both when learning a single global model [46] and when personalizing the model to subsets of users [4]. We do note that the overhead of those methods can be significant.

Decentralized Peer Sampling. Brahms [6], Basalt [2] and PeerSampling [20] provide uniformly random samples without network-wide synchronization. However, to the best of our knowledge, MoDEST is the first decentralized sampling mechanism that ensures samples are mostly consistent, in the presence of nodes joining, leaving, and crashing.

6 Conclusions

We have presented MoDEST, a decentralized learning system that adopts the sampling approach of FL to decentralizing the server over multiple nodes and limiting the number of nodes involved at each training round thus reducing the communication costs compared to DL. At the core of MoDEST is our novel approach to derive mostly-consistent samples by nodes themselves. In each round, participating nodes determine the next sample and send their updated models to a smaller subset of aggregators within this sample. Aggregators aggregate incoming models in parallel and push the aggregated model to nodes in the next sample. This approach effectively delegates the responsibility of the server used in FL to participating nodes and makes MoDEST robust against

failing nodes. Our extensive experimental evaluation reveals that MoDeST, for most learning tasks, converges faster than DL and FL, incurs modest communication overhead ranging from 0.4% to 22.2%, significantly improves load balancing amongst nodes compared to FL, and ensures liveness in the presence of unresponsive nodes.

A natural future research avenue is to enhance MoDeST to account for Byzantine nodes that attempt to undermine the learning process by leveraging the sampling mechanism to implement an accounting process. This would be a next step towards the ambitious goal of deploying decentralized learning systems at scale and in open settings.

Acknowledgments

We wish to thank the software development team of the Distributed Systems Group for maintaining the experiment infrastructure we used in this paper, and the Distributed Systems Group and TU Delft for lending their cluster for the experiments performed in this paper.

References

- [1] 2017. <https://ai.googleblog.com/2017/04/federated-learning-collaborative.html>
- [2] Alex Auvolat, Yérom-David Bromberg, Davide Frey, and François Taïani. 2021. BASALT: A Rock-Solid Foundation for Epidemic Consensus Algorithms in Very Large, Very Open Networks. *arXiv preprint arXiv:2102.04063* (2021).
- [3] Xianglin Bao, Cheng Su, Yan Xiong, Wenchao Huang, and Yifei Hu. 2019. Flchain: A blockchain for auditable federated learning with trust and incentive. In *2019 5th International Conference on Big Data Computing and Communications (BIGCOM)*. IEEE, 151–159.
- [4] Jossekin Beilharz, Bjarne Pfitzner, Robert Schmid, Paul Geppert, Bert Arnrich, and Andreas Polze. 2021. Implicit Model Specialization through Dag-Based Decentralized Federated Learning. In *Proceedings of the 22nd International Middleware Conference* (Québec city, Canada) (*Middleware '21*). Association for Computing Machinery, New York, NY, USA, 310–322. <https://doi.org/10.1145/3464298.3493403>
- [5] Aurélien Bellet, Anne-Marie Kermarrec, and Erick Lavoie. 2021. D-Cliques: Compensating NonIIDness in Decentralized Federated Learning with Topology. *arXiv preprint arXiv:2104.07365* (2021).
- [6] Edward Bortnikov, Maxim Gurevich, Idit Keidar, Gabriel Kliot, and Alexander Shraer. 2009. Brahms: Byzantine resilient random membership sampling. *Computer Networks* 53, 13 (2009), 2340–2359.
- [7] Theodora S Brisimi, Ruidi Chen, Theofanie Mela, Alex Olshevsky, Ioannis Ch Paschalidis, and Wei Shi. 2018. Federated learning of predictive models from federated electronic health records. *International journal of medical informatics* 112 (2018), 59–67.
- [8] Sebastian Caldas, Sai Meher Karthik Duddu, Peter Wu, Tian Li, Jakub Konečný, H Brendan McMahan, Virginia Smith, and Ameet Talwalkar. 2019. Leaf: A benchmark for federated settings. In *2nd Intl. Workshop on Federated Learning for Data Privacy and Confidentiality (FL-NeurIPS)*.
- [9] Mingqing Chen, Rajiv Mathews, Tom Ouyang, and Françoise Beaufays. 2019. Federated learning of out-of-vocabulary words. *arXiv preprint arXiv:1903.10635* (2019).
- [10] Mingzhe Chen, H Vincent Poor, Walid Saad, and Shuguang Cui. 2020. Wireless Communications for Collaborative Federated Learning in the Internet of Things. *arXiv preprint arXiv:2006.02499* (2020).
- [11] Mingqing Chen, Ananda Theertha Suresh, Rajiv Mathews, Adeline Wong, Cyril Allauzen, Françoise Beaufays, and Michael Riley. 2019. Federated learning of N-gram language models. *arXiv preprint arXiv:1910.03432* (2019).
- [12] John R Douceur. 2002. The sybil attack. In *International workshop on peer-to-peer systems*. Springer, 251–260.
- [13] Cynthia Dwork, Nancy Lynch, and Larry Stockmeyer. 1988. Consensus in the presence of partial synchrony. *Journal of the ACM (JACM)* 35, 2 (1988), 288–323.
- [14] GroupLens. 2021. MovieLens Datasets. <https://grouplens.org/datasets/movielens/>
- [15] Jenny Hamer, Mehryar Mohri, and Ananda Theertha Suresh. 2020. Fedboost: A communication-efficient algorithm for federated learning. In *International Conference on Machine Learning*. PMLR, 3973–3983.
- [16] Andrew Hard, Kanishka Rao, Rajiv Mathews, Swaroop Ramaswamy, Françoise Beaufays, Sean Augenstein, Hubert Eichner, Chloé Kiddon, and Daniel Ramage. 2018. Federated learning for mobile keyboard prediction. *arXiv preprint arXiv:1811.03604* (2018).
- [17] István Hegedűs, Gábor Danner, and Márk Jelasity. 2021. Decentralized learning works: An empirical comparison of gossip learning and federated learning. *J. Parallel and Distrib. Comput.* 148 (2021), 109–124.
- [18] Kevin Hsieh, Amar Phanishayee, Onur Mutlu, and Phillip Gibbons. 2020. The non-iid data quagmire of decentralized machine learning. In *International Conference on Machine Learning*. PMLR, 4387–4398.
- [19] Dzmitry Huba, John Nguyen, Kshitiz Malik, Ruiyu Zhu, Mike Rabbat, Ashkan Yousefpour, Carole-Jean Wu, Hongyuan Zhan, Pavel Ustinov, Harish Srinivas, Kaikai Wang, Anthony Shoumikhin, Jesik Min, and Mani Malek. 2022. PAPAYA: Practical, Private, and Scalable Federated Learning. In *Proceedings of Machine Learning and Systems*, D. Marculescu, Y. Chi, and C. Wu (Eds.), Vol. 4, 814–832. <https://proceedings.mlsys.org/paper/2022/file/f340f1b1f65b6df5b5e3f94d95b11daf-Paper.pdf>
- [20] Márk Jelasity, Spyros Voulgaris, Rachid Guerraoui, Anne-Marie Kermerrec, and Maarten Van Steen. 2007. Gossip-based peer sampling. *ACM Transactions on Computer Systems (TOCS)* 25, 3 (2007), 8–es.
- [21] Peter Kairouz, H Brendan McMahan, Brendan Avent, Aurélien Bellet, Mehdi Bennis, Arjun Nitin Bhagoji, Kallista Bonawitz, Zachary Charles, Graham Cormode, Rachel Cummings, et al. 2021. Advances and Open Problems in Federated Learning. *Foundations and Trends® in Machine Learning* 14, 1–2 (2021), 1–210.
- [22] Hyesung Kim, Jihong Park, Mehdi Bennis, and Seong-Lyun Kim. 2018. On-device federated learning via blockchain and its latency analysis. *arXiv preprint arXiv:1808.03949* (2018).
- [23] Anastasia Koloskova, Nicolas Loizou, Sadra Boreiri, Martin Jaggi, and Sebastian Stich. 2020. A Unified Theory of Decentralized SGD with Changing Topology and Local Updates. In *Proceedings of the 37th International Conference on Machine Learning (Proceedings of Machine Learning Research, Vol. 119)*, Hal Daumé III and Aarti Singh (Eds.). PMLR, 5381–5393. <https://proceedings.mlr.press/v119/koloskova20a.html>
- [24] Anastasia Koloskova, Sebastian Stich, and Martin Jaggi. 2019. Decentralized Stochastic Optimization and Gossip Algorithms with Compressed Communication. In *Proceedings of the 36th International Conference on Machine Learning (Proceedings of Machine Learning Research, Vol. 97)*, Kamalika Chaudhuri and Ruslan Salakhutdinov (Eds.). PMLR, 3478–3487. <https://proceedings.mlr.press/v97/koloskova19a.html>
- [25] Lingjing Kong, Tao Lin, Anastasia Koloskova, Martin Jaggi, and Sebastian Stich. 2021. Consensus Control for Decentralized Deep Learning. In *Proceedings of the 38th International Conference on Machine Learning (Proceedings of Machine Learning Research, Vol. 139)*, Marina Meila and Tong Zhang (Eds.). PMLR, 5686–5696. <https://proceedings.mlr.press/v139/kong21a.html>
- [26] Yehuda Koren, Robert Bell, and Chris Volinsky. 2009. Matrix Factorization Techniques for Recommender Systems. *Computer* 42, 8 (aug 2009), 30–37. <https://doi.org/10.1109/MC.2009.263>

[27] Alex Krizhevsky. 2009. Learning Multiple Layers of Features from Tiny Images. <https://www.cs.toronto.edu/~kriz/learning-features-2009-TR.pdf>. (2009).

[28] Fan Lai, Xiangfeng Zhu, Harsha V. Madhyastha, and Mosharaf Chowdhury. 2021. Oort: Efficient Federated Learning via Guided Participant Selection. In *15th USENIX Symposium on Operating Systems Design and Implementation (OSDI 21)*. USENIX Association, 19–35. <https://www.usenix.org/conference/osdi21/presentation/lai>

[29] Tian Li, Anit Kumar Sahu, Manzil Zaheer, Maziar Sanjabi, Ameet Talwalkar, and Virginia Smith. 2020. Federated Optimization in Heterogeneous Networks. In *MLSys*. <https://proceedings.mlsys.org/paper/2020/file/38af86134b65d0f10fe33d30dd76442e-Paper.pdf>

[30] Xiangru Lian, Ce Zhang, Huan Zhang, Cho-Jui Hsieh, Wei Zhang, and Ji Liu. 2017. Can decentralized algorithms outperform centralized algorithms? a case study for decentralized parallel stochastic gradient descent. *Advances in Neural Information Processing Systems* 30 (2017).

[31] Xiangru Lian, Ce Zhang, Huan Zhang, Cho-Jui Hsieh, Wei Zhang, and Ji Liu. 2017. Can Decentralized Algorithms Outperform Centralized Algorithms? A Case Study for Decentralized Parallel Stochastic Gradient Descent. In *NIPS*.

[32] Songtao Lu, Yawen Zhang, and Yunlong Wang. [n. d.]. Decentralized federated learning for electronic health records. In *2020 54th Annual Conference on Information Sciences and Systems (CISS)*. IEEE, 1–5.

[33] Yunlong Lu, Xiaohong Huang, Yueyue Dai, Sabita Maharjan, and Yan Zhang. 2019. Blockchain and federated learning for privacy-preserved data sharing in industrial IoT. *IEEE Transactions on Industrial Informatics* 16, 6 (2019), 4177–4186.

[34] Umer Majeed and Choong Seon Hong. 2019. FLchain: Federated learning via MEC-enabled blockchain network. In *2019 20th Asia-Pacific Network Operations and Management Symposium (APNOMS)*. IEEE, 1–4.

[35] Brendan McMahan, Eider Moore, Daniel Ramage, Seth Hampson, and Blaise Aguera y Arcas. 2017. Communication-Efficient Learning of Deep Networks from Decentralized Data. In *Proceedings of the 20th International Conference on Artificial Intelligence and Statistics (Proceedings of Machine Learning Research, Vol. 54)*, Aarti Singh and Jerry Zhu (Eds.). PMLR, 1273–1282.

[36] Dinh C Nguyen, Ming Ding, Quoc-Viet Pham, Pubudu N Pathirana, Long Bao Le, Aruna Seneviratne, Jun Li, Dusit Niyato, and H Vincent Poor. 2021. Federated learning meets blockchain in edge computing: Opportunities and challenges. *IEEE Internet of Things Journal* (2021).

[37] John Nguyen, Kshitiz Malik, Hongyuan Zhan, Ashkan Yousefpour, Mike Rabbat, Mani Malek, and Dzmitry Huba. 2022. Federated Learning with Buffered Asynchronous Aggregation. In *Proceedings of The 25th International Conference on Artificial Intelligence and Statistics (Proceedings of Machine Learning Research, Vol. 151)*, Gustau Camps-Valls, Francisco J. R. Ruiz, and Isabel Valera (Eds.). PMLR, 3581–3607. <https://proceedings.mlr.press/v151/nguyen22b.html>

[38] Solmaz Niknam, Harpreet S Dhillon, and Jeffrey H Reed. 2020. Federated learning for wireless communications: Motivation, opportunities, and challenges. *IEEE Communications Magazine* 58, 6 (2020), 46–51.

[39] Róbert Ormándi, István Hegedűs, and Márk Jelasity. 2013. Gossip learning with linear models on fully distributed data. *Concurrency and Computation: Practice and Experience* 25, 4 (2013), 556–571.

[40] Adam Paszke, Sam Gross, Francisco Massa, Adam Lerer, James Bradbury, Gregory Chanan, Trevor Killeen, Zeming Lin, Natalia Gimelshein, Luca Antiga, et al. 2019. Pytorch: An imperative style, high-performance deep learning library. *Advances in neural information processing systems* 32 (2019).

[41] Shiva Raj Pokhrel and Jinho Choi. 2020. Federated learning with blockchain for autonomous vehicles: Analysis and design challenges. *IEEE Transactions on Communications* 68, 8 (2020), 4734–4746.

[42] Michel Raynal. 1992. About logical clocks for distributed systems. *ACM SIGOPS Operating Systems Review* 26, 1 (1992), 41–48.

[43] Sashank J. Reddi, Zachary Charles, Manzil Zaheer, Zachary Garrett, Keith Rush, Jakub Konečný, Sanjiv Kumar, and Hugh Brendan McMahan. 2021. Adaptive Federated Optimization. In *International Conference on Learning Representations*. <https://openreview.net/forum?id=LkFG3IB13U5>

[44] Nicola Rieke, Jonny Hancox, Wenqi Li, Fausto Milletari, Holger Roth, Shadi Albarqouni, Spyridon Bakas, Mathieu N Galtier, Bennett Landman, and Klaus Maier-Hein. 2020. The future of digital health with federated learning. *arXiv preprint arXiv:2003.08119* (2020).

[45] Max Ryabinin, Eduard Gorbunov, Vsevolod Plokhotnyuk, and Gennady Pekhimenko. 2021. Moshpit SGD: Communication-efficient decentralized training on heterogeneous unreliable devices. *Advances in Neural Information Processing Systems* 34 (2021).

[46] Robert Schmid, Bjarne Pfitzner, Jossekin Beilharz, Bert Arnrich, and Andreas Polze. 2020. Tangle ledger for decentralized learning. In *2020 IEEE International Parallel and Distributed Processing Symposium Workshops (IPDPSW)*. IEEE, 852–859.

[47] William Schneble and Geethapriya Thamilarasu. [n. d.]. Attack Detection Using Federated Learning in Medical Cyber-Physical Systems. ([n. d.]).

[48] Khe Chai Sim, Françoise Beaufays, Arnaud Benard, Dhruv Guliani, Andreas Kabel, Nikhil Khare, Tamar Lucassen, Petr Zadrazil, Harry Zhang, and Leif Johnson. [n. d.]. Personalization of end-to-end speech recognition on mobile devices for named entities. In *2019 IEEE Automatic Speech Recognition and Understanding Workshop (ASRU)*. IEEE, 23–30.

[49] K Sollins. 1992. *The TFTP protocol (revision 2)*. Technical Report. STD 33, RFC 1350, MIT.

[50] Konstantin Sozinov, Vladimir Vlassov, and Sarunas Girdzijauskas. [n. d.]. Human Activity Recognition Using Federated Learning. In *2018 IEEE Intl Conf on Parallel & Distributed Processing with Applications, Ubiquitous Computing & Communications, Big Data & Cloud Computing, Social Computing & Networking, Sustainable Computing & Communications (ISPA/IUCC/BDCloud/SocialCom/SustainCom)*. IEEE, 1103–1111.

[51] Tribler Team. [n. d.]. IPv8 Networking Library. <https://github.com/tribler/py-ipv8>.

[52] WonderNetwork. [n. d.]. Global Ping Statistics. <https://wondernetwork.com/pings>. Accessed: 2022-05-12.

[53] Bicheng Ying, Kun Yuan, Yiming Chen, Hanbin Hu, Pan Pan, and Wotao Yin. 2021. Exponential graph is provably efficient for decentralized deep training. *Advances in Neural Information Processing Systems* 34 (2021), 13975–13987.